

Durham Research Online

Deposited in DRO:

21 January 2015

Version of attached file:

Published Version

Peer-review status of attached file:

Peer-reviewed

Citation for published item:

Knight, R. and Piette, C.E. and Page, H. and Walters, D. and Marozzi, E. and Nardini, M. and Stringer, S. and Jeffery, K.J. (2014) 'Weighted cue integration in the rodent head direction system.', *Philosophical transactions of the Royal Society B : biological sciences.*, 369 (1635). p. 20120512.

Further information on publisher's website:

<https://doi.org/10.1098/rstb.2012.0512>

Publisher's copyright statement:

© 2013 The Authors. Published by the Royal Society under the terms of the Creative Commons Attribution License <http://creativecommons.org/licenses/by/3.0/>, which permits unrestricted use, provided the original author and source are credited.

Additional information:

Use policy

The full-text may be used and/or reproduced, and given to third parties in any format or medium, without prior permission or charge, for personal research or study, educational, or not-for-profit purposes provided that:

- a full bibliographic reference is made to the original source
- a [link](#) is made to the metadata record in DRO
- the full-text is not changed in any way

The full-text must not be sold in any format or medium without the formal permission of the copyright holders.

Please consult the [full DRO policy](#) for further details.



Cite this article: Knight R, Piette CE, Page H, Walters D, Marozzi E, Nardini M, Stringer S, Jeffery KJ. 2014 Weighted cue integration in the rodent head direction system. *Phil. Trans. R. Soc. B* **369**: 20120512. <http://dx.doi.org/10.1098/rstb.2012.0512>

One contribution of 24 to a Theo Murphy Meeting Issue ‘Space in the brain: cells, circuits, codes and cognition’.

Subject Areas:

behaviour, cognition, computational biology, neuroscience, theoretical biology

Keywords:

head direction cells, sensory cue integration, path integration, attractor dynamics, vision, vestibular system

Author for correspondence:

Kathryn J. Jeffery
e-mail: k.jeffery@ucl.ac.uk

Electronic supplementary material is available at <http://dx.doi.org/10.1098/rstb.2012.0512> or via <http://rstb.royalsocietypublishing.org>.

Weighted cue integration in the rodent head direction system

Rebecca Knight¹, Caitlin E. Piette¹, Hector Page², Daniel Walters², Elizabeth Marozzi¹, Marko Nardini³, Simon Stringer² and Kathryn J. Jeffery¹

¹Division of Psychology and Language Sciences, Department of Cognitive, Perceptual and Brain Sciences, Institute of Behavioural Neuroscience, University College London, 26 Bedford Way, London WC1H 0AP, UK

²Department of Experimental Psychology, University of Oxford, South Parks Road, Oxford OX1 3UD, UK

³Department of Visual Neuroscience, Institute of Ophthalmology, 11-43 Bath Street, London EC1V 9EL, UK

How the brain combines information from different sensory modalities and of differing reliability is an important and still-unanswered question. Using the head direction (HD) system as a model, we explored the resolution of conflicts between landmarks and background cues. Sensory cue integration models predict averaging of the two cues, whereas attractor models predict capture of the signal by the dominant cue. We found that a visual landmark mostly captured the HD signal at low conflicts; however, there was an increasing propensity for the cells to integrate the cues thereafter. A large conflict presented to naive rats resulted in greater visual cue capture (less integration) than in experienced rats, revealing an effect of experience. We propose that weighted cue integration in HD cells arises from dynamic plasticity of the feed-forward inputs to the network, causing within-trial spatial redistribution of the visual inputs onto the ring. This suggests that an attractor network can implement decision processes about cue reliability using simple architecture and learning rules, thus providing a potential neural substrate for weighted cue integration.

1. Introduction

The ‘sense of direction’ is supported by the limbic head direction (HD) cells, which respond to allocentric HD (that is, direction of the head with respect to the world) regardless of the animal’s location in an environment [1,2]. Each HD cell is tuned to a single head orientation, and when the head is directed to the cell’s preferred firing direction the cell fires at maximum [1]. Many studies have illustrated that the HD system is strongly reliant on external landmark cues in order to determine heading direction [3–5]. However, this reliance is variable, depending upon the type of external cue, the location of that cue in the environment, the prior experience of the cue and the duration of exposure to it. HD cells also maintain their firing in the dark, albeit with a drift in preferred firing direction [3]. The ability of HD cells to maintain stable firing when landmarks are not visible suggests that the cells can rely on self-motion information to sustain the signal when landmark information is unavailable [3,6,7].

Theoretical models have proposed that landmark and self-motion cues interact by convergence onto an interconnected network of cells known as a ring attractor [8,9]. This is a hypothetical network of HD cells in which activity moves smoothly from one set of cells to the next via recurrent connections between the cells, as the animal turns through space, thus keeping the signal constantly and dynamically updated (see the electronic supplementary material and [10] for a more detailed explanation). The influence of self-motion cues in shifting activity around this conceptual ‘ring’ may be supported by weak environmental information, such as static auditory, olfactory and other transiently stable cues, collectively producing a set of cues that we refer to here as ‘background cues’ that serve to align the animal’s internal representation of HD with the external world.

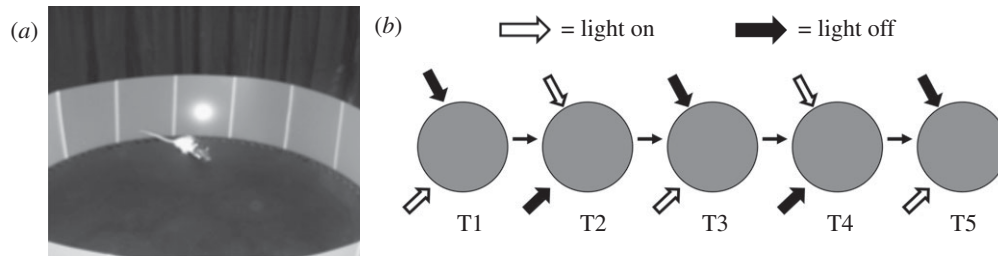


Figure 1. The experimental protocol. (a) Photograph of the apparatus, showing the light cue behind the translucent wall of the arena. (b) A schematic drawing of the experimental protocol for the 60° conflict condition from Experiment 1. The position of the two lights is shown by the thick arrows (white arrows represent when the light is on and black arrows represent when the light is off). Each trial lasted for 4 min and between each trial the rat foraged in darkness for 10 s (thin arrows).

The HD signal may drift or become unreliable over time and can be periodically corrected, or ‘reset’, by the influence of landmarks. When landmarks and background cues conflict (for example, when looking up and seeing a familiar landmark in an unexpected direction), then the system needs to decide which cue(s) to ‘trust’ (did the landmark move or am I disoriented?) and by how much. This is a classic case of sensory cue integration, the general neural mechanisms of which are unknown at present. HD cells provide a useful model system with which to explore such mechanisms because they produce a simple and easily measured output along a single dimension (direction).

A number of previous studies have examined how HD cells respond to cue conflict [3,4,7,11–18]. Such studies have suggested that there is visual capture (dominance of visual landmark control) when conflicts are small but capture by the background cues when conflicts are large [19,20], a switch that has been attributed to the dynamics of the ring attractor. In order to examine this process in more detail, we therefore examined HD cell activity when a visual directional landmark conflicted with background cues by angular amounts that steadily increased across days. We predicted that we would see complete (or almost complete) cue capture, by either the background cues or the landmark, with a transition from one cue to the other at a certain ‘break point’. However, as we show here, this did not happen: the cells instead adopted intermediate states. This finding is not consistent with standard attractor dynamics because the activity should always be ‘dragged’ around the ring towards the strongest cue, until it aligns with the cue and cannot move any further. The finding of intermediate states, where activity shifts to a point short of the strongest cue, implies that some additional process must be occurring. We propose that this compromise behaviour could be mediated by plasticity in the inputs, such that the strongest cue actually shifts its connections with the ring attractor. We show how such short-term plasticity in an attractor network might provide a mechanism for reliability-weighted cue averaging, and furthermore that longer-term plasticity in the same inputs could account for new learning about cue reliability.

2. Material and methods

(a) Subjects

Subjects were nine adult male Lister Hooded rats (six in Experiment 1 and three in Experiment 2), weighing between 250 and 400 g at the time of surgery. The rats in Experiment 1 were non-naïve to the recording setting, having been recorded in another simultaneous experiment examining the influence of geometry

on HD cells during disorientation and non-disorientation conditions [21]. In this experiment, they undertook foraging trials in environments of varying geometry that were rotated from trial to trial—the animals were thus familiar with the curtained enclosure and with the foraging procedure, and possibly with uncontrolled distal auditory and olfactory cues. The rats in Experiment 2 were naïve to the environment at the start of recording. The rats were housed individually (11:11 light:dark, with 1 h ($\times 2$) simulated dawn/dusk) on a food-restricted diet (sufficient to maintain 90% of free-feeding weight) with ad libitum access to water. In Experiment 1, the rats were implanted with recording electrodes in anterior thalamus (ADN; $n = 2$), postsubiculum (PoS; $n = 2$) or retrosplenial cortex (RSC; $n = 2$). In Experiment 2, all electrodes were located in RSC. All procedures were licensed by the UK Home Office subject to the restrictions and provisions contained in the Animals (Scientific Procedures) Act 1986.

(b) Electrode implantation

All rats were implanted at the start of the experiment with 4-tetrode electrode bundles, using methods previously described [21]. In Experiment 1, two rats (R321 and R344) were implanted in the PoS (bregma coordinates: 6.7 AP, 2.8 ML, 1.6 DV), two rats (R409 and R410) were implanted in the ADN (bregma coordinates: –1.8 AP, 1.4 ML, –2.1 DV), and two rats (R1696 and R1704) were implanted in the RSC (bregma coordinates: –5.5/–6.3 AP, 1.3/1.5 ML, –1.2/–2.3 DV). In Experiment 2, three rats (R517, R518 and R520) were implanted in the RSC (bregma coordinates: –5.4 AP, ± 0.6 ML, –1.2/2.3 DV). Once the electrodes were in place, the metallic guide cannula was pulled down over the remaining exposed wire. Sterile Vaseline (Lever Fabergé, Germany) was placed around the bottom of the guide cannula and the implant was then attached to the skull with dental acrylic. The animals were then monitored periodically until they awoke. All animals were given at least one week to recover following the surgery, during which time they were given ad libitum access to food and water. They were given meloxicam (Metacam, Boehringer Ingelheim) for the first 3 days postsurgery, administered in fruit jelly (0.15 ml per 0.85 ml portion of jelly).

(c) Apparatus

A circular wooden platform 1.2 m in diameter was located in the centre of a curtained enclosure 2 m in diameter (figure 1a) and positioned 50 cm from the floor on a box. Beneath the platform, inside the box, was a detuned radio generating white noise, to mask auditory cues. The walls of the arena were made of translucent flexible plastic that allowed the presentation of a landmark in the form of a bright spot, created by a flashlight positioned on a clamp stand behind the wall. As all main lights were switched off during the experiment, the flashlight was the only salient polarizing landmark. During cue conflict trials, two lights were used so the light could easily move location without the need

to physically move the flashlights. Only one light was ever switched on at a time.

(d) Screening and recording procedures

Screening for cells commenced one week after surgery and took place in a room separate from the actual experimental room, to minimize the learning of extraneous cues in the recording environment by the rats. Screening and recording were done using multi-channel recording equipment (DacqUSB, Axona Ltd). The rats were connected to the recording device via lightweight wires attached to the microdrive. The potentials recorded on each of the 16 electrodes of the four tetrodes were passed through AC-coupled, unity gain operational amplifiers mounted on the rat's head (headstage) and fed to the recording system. The signal was amplified (approx. 20 000 times), bandpass filtered (500 Hz–7 kHz), and then collected and stored on a computer for offline analysis. Each of the four wires of one tetrode was recorded differentially with respect to one of the wires of one of the other tetrodes in order to subtract common noise (e.g. chewing artefact).

In order to determine the direction of the rat's head, a directional headstage was used in which two LEDs of differing sizes (one large and one small), spaced 8 cm apart, were attached to the headstage. The angle of the lights with respect to the head was noted for each implant. The lights were detected by a video camera attached to the ceiling, and Dacq hardware and software used to extract position and HD, respectively. During screening, rats were encouraged to sample the space by foraging for sweet cereal while the oscilloscope was monitored to check for unit spiking. If no single-cell activity was present, the electrodes were lowered by approximately 50 μm . If no HD cells were found, rats were returned to their home cage for at least 4 h before the next screening session. If HD cells were found, a recording session was run. Only one 5-trial session (described below) was run on a given day, with sessions of increasing conflict size run on successive days where possible, until the cell was lost.

When a well-isolated and stable HD cell was found, the rat was taken into the experimental room in an opaque carrying box and placed on a raised holding box outside the curtained enclosure, in order to acclimatize to the room for 5 min. During this time, the rat was connected to the recording device and returned to the box, which was then carried into the enclosure through one of three joins in the curtains, and placed in a pseudo-random location on the floor. After 1 min, the rat was taken out of the holding box and placed at the centre of the platform.

On the first session, the environment was set up so that one flashlight was on while the second flashlight, which was switched off, was placed 20° away from the first light, in a clockwise direction. This direction remained constant for each rat, except in the probe trials when the direction was reversed (beginning anticlockwise). Recording began when the rat was placed in the environment, whereupon it began foraging for food scattered across the arena surface by the experimenter. After 4 min of recording, the original light was switched off, signalling the end of trial one, and the rat was left in darkness for 10 s before the second light, located at a given angular distance from the first, was switched on for a further 4 min of recording. This protocol was then repeated so that during each session there were five trials, three with the light in the original location and two with it in its rotated location (figure 1b). Cell activity was continuously recorded during this whole time period (20 min and 40 s). At no point in a recording session was the rat disoriented or the platform cleaned. Therefore, the rat could have used olfactory cues from the platform, or vestibular information, to orient itself. These vestibular information and olfactory cues (collectively called 'background cues') remained intact throughout the session.

For the subsequent session, on a different day, both lights were moved to a new location around the arena, so as to prevent

the rat from forming a stable association with distant auditory and olfactory cues that would interfere with landmark control. For Experiment 1, the angular separation between the lights was increased by 20° from the previous day, up to a maximum of 180°, while for Experiment 2 it remained constant at 140°.

(e) Single neuron analysis

Cluster-cutting software (Tint, Axona Ltd) was used to analyse the data offline. Clusters were generated based on the peak-to-peak amplitudes of the spike traces for each pair of electrodes, and separated manually. Cells with a peak firing rate of less than 1.0 Hz across the session were excluded from further analysis. For the remainder, polar plots of spike rate against HD were created in Tint, using a smoothing kernel of five bins, in order to determine each cell's directional firing preference.

Four parameters were used to assess the characteristics of each HD cell's activity: mean firing direction, peak firing rate, resultant vector length and directional firing range (tuning curve width). In order to calculate these parameters, the spike count for each direction across the whole trial was recorded along with the dwell time for each direction (the amount of time the rat faced each direction). In MATLAB (Mathworks, Natick, MA, USA), the spike count and dwell time were then divided into 60 six-degree bins. To calculate the firing rate count for each directional bin, the spike count was divided by the dwell time. Resultant vector lengths (see below) were calculated on this unsmoothed firing rate data. The mean firing direction was calculated by smoothing the firing rate using a kernel of 5°, and then taking a weighted circular average of the smoothed firing rate count.

The preferred firing direction was also calculated by finding the directional bin with the highest average firing rate, and thus can be equated to the mode of the tuning curve. As the mode does not take into account all data points, the analysis in the results section uses the mean firing direction.

In order to assess the degree to which the data deviated from the circular mean, resultant vector lengths were calculated on unsmoothed data. Thus, resultant vector lengths ('*R*') measure the circular spread of data. In order to calculate the resultant vector length, the circular mean value of the angular data was calculated. This was done by transforming the angular data into vectors

$$r_i = \begin{pmatrix} \cos \alpha_i \\ \sin \alpha_i \end{pmatrix}.$$

These vectors were then averaged to produce a mean resultant vector ('*r*')

$$\bar{r} = \frac{1}{N} \sum_i r_i.$$

The absolute value of *r* gave the length of this mean resultant vector ('*R*'):

$$R = \|\bar{r}\|.$$

Resultant vector lengths ('*R*') range from 0 to 1. Resultant vector length '*R*' values that are closer to 1 indicate less variance in the dataset. A Rayleigh test (z-test statistic) can then be used to see how large the '*R*' values (resultant vector lengths) must be to indicate a non-uniform distribution [14]. A significant Rayleigh test indicates that the distribution is clustered around a particular direction. HD cells that had an '*R*' value of less than 0.3 within a given session were excluded [22].

Analysis of HD cell mean firing direction was performed using circular statistics, examining mean values of cells that had been recorded simultaneously, i.e. as an ensemble (ranging from 1 to 3 cells). All circular analysis was also done using the CircStat Matlab toolbox [23], with a subset of trials checked by

hand, yielding identical values. In order to analyse the rotation of HD cells between the standard and shifted-light conditions, the circular mean direction of cells in each light-shift trial was subtracted from the circular mean direction of cells in the preceding standard trial, to provide a measure of how far the ensemble rotated. The mean of these two rotations was taken to be the mean ensemble shift for that session. These mean shifts were then subtracted from the predicted angle of shift (based on how much the light had rotated) to produce absolute deviations from expected rotation. The mean vector length of absolute deviations for each condition was calculated. The Rayleigh test [23] was then used to determine whether these absolute mean deviations clustered around a particular direction. Circular inferential statistics [23] were used to compare absolute mean deviation values against zero (the predicted deviation given perfect light-following), using a one-sample test. The Watson–Williams test (the circular analogue of the one-way ANOVA) was used to calculate the main effects of circular mean rotation across session.

In order to measure the width of the HD tuning curve (the firing rate versus HD plot) the two sides of the curve were linearized using the method of Taube *et al.* [1]. This was done by selecting (by eye) a point adjacent to the peak and another point on the curve close to the base, and drawing a line through these that was extrapolated down to the x -axis. The distance between the x -intercepts of the two lines was taken to be the width of the tuning curve.

(f) Histological analysis

Once the experiments were finished, the rats were then deeply anaesthetized with isoflurane induction followed by sodium pentobarbital injection. When breathing ceased they were transcardially perfused with saline followed by paraformaldehyde (4%). The brains were removed and stored in paraformaldehyde (4%) for at least one week before being sliced into 40 μ m sections on a freezing microtome. The sections were then mounted and stained with Cresyl violet, and the slides were observed under a DM750 microscope (Leica, UK) in order to determine the site of the electrode track, which was verified using a rat brain atlas [24].

3. Results

(a) Experiment 1

A total of 17 individual HD cells, in eight ensembles of one to three cells in each, were recorded from six rats during 54 sessions of 270 trials. These 17 HD cells met the inclusion criteria of having a peak firing rate of more than 1.0 Hz and a mean vector length (' R ') of more than 0.3. Across all 17 cells, the average peak firing rate was 16.37 Hz (± 2.25), the average firing range was 120.8° (± 4.86) and the average ' R ' value was 0.54.

(i) Cue conflict trials

When the light cue was moved, thus generating a conflict between the light and the background cues, cells generally rotated their mean firing direction in the same direction. An example of the response of a single HD cell to rotation of the light by 120° is shown in figure 2.

If multiple cells were recorded in a session, the average mean shift was calculated, because HD cells from a single animal always act in concert and react together to environmental changes [1]. All subsequent analysis was performed on ensemble data using the CircStat Matlab toolbox. The pattern of response for the cells from the six animals, across the range of conflicts, is shown in figure 3.

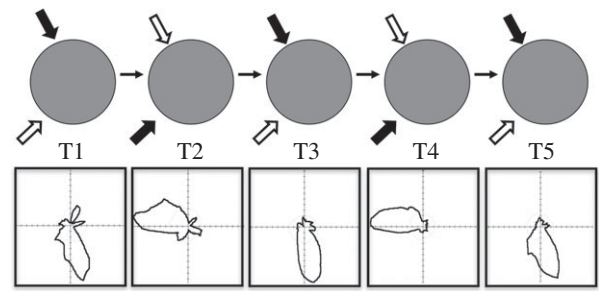


Figure 2. Five polar plots of one cell recorded from Rat 321 (PoS implant) during 120° light conflict session in Experiment 1. The white (light on) and black (light off) arrows represent the two torches separated by 120°. Note that the HD cell in this example rotates by approximately 110° between trials, in the same direction as the light.

These data showed an interesting relationship between the amount of conflict and the responses of the cells (figure 3 and table 1). For conflicts between 20° and 100°, there was a general trend for the cells to follow the light fairly closely except for an absolute mean deviation or 'undershoot' that was approximately constant. The variation within the data also increased with an increase in light rotations, which is reflected in the standard deviation values and vector length ' R ' values. However, column six of table 1 shows that all data points are significantly clustered (at an α -level of 0.05* or 0.001***) within each of the light rotation sessions (Rayleigh test, see table 1). This suggests that all the recorded HD cells rotated their firing by similar amounts when exposed to a given light conflict. The comparison between the actual mean ensemble shift for each session and the expected shift (light rotation) is illustrated in figure 4. Figure 4 also shows the mean firing rotation for each session when data from only the last 2 min of each trial were used. It can be seen that the mean firing shift for the latter half of each trial is very similar to the mean firing shift for the entire trial, indicating that the mean firing direction had stabilized within at least the first 2 min of each trial.

Figure 4 shows that the mean shift in cells steadily increased with the angular rotation of the light (i.e. the cells followed the light), with a slight undershoot, up until the point at which the light shifted by more than 120°, at which point the angular separation between the shift of the light and the shift of the cells' preferred firing direction began to steadily increase. This pattern in the data was quantified by calculating the amount of shift in the mean firing direction as a percentage of the actual light rotation (table 1). A Watson–Williams test revealed a main effect of session ($F_{8,45} = 4.86$, $p < 0.001$). Post hoc tests were then applied to these data, to determine (i) whether the mean firing direction rotated significantly less than the light and (ii) rotated significantly more than would be predicted by the background cues (i.e. more than zero). This analysis showed that the deviation in mean firing rotation from the actual light rotation was significantly greater than zero for all conflicts, except 120° (table 2, column 3).

This is consistent with the under-rotation of HD cells' mean firing direction that has been reported in the literature, which are typically around 15°–20° [3,25]. In comparing the mean firing shift with the unrotated background cues, we found that the mean firing shifts for all sessions were also significantly different from zero (table 2, column 5). This indicates that on average cells showed some rotation during all sessions and were not controlled completely by either cue.

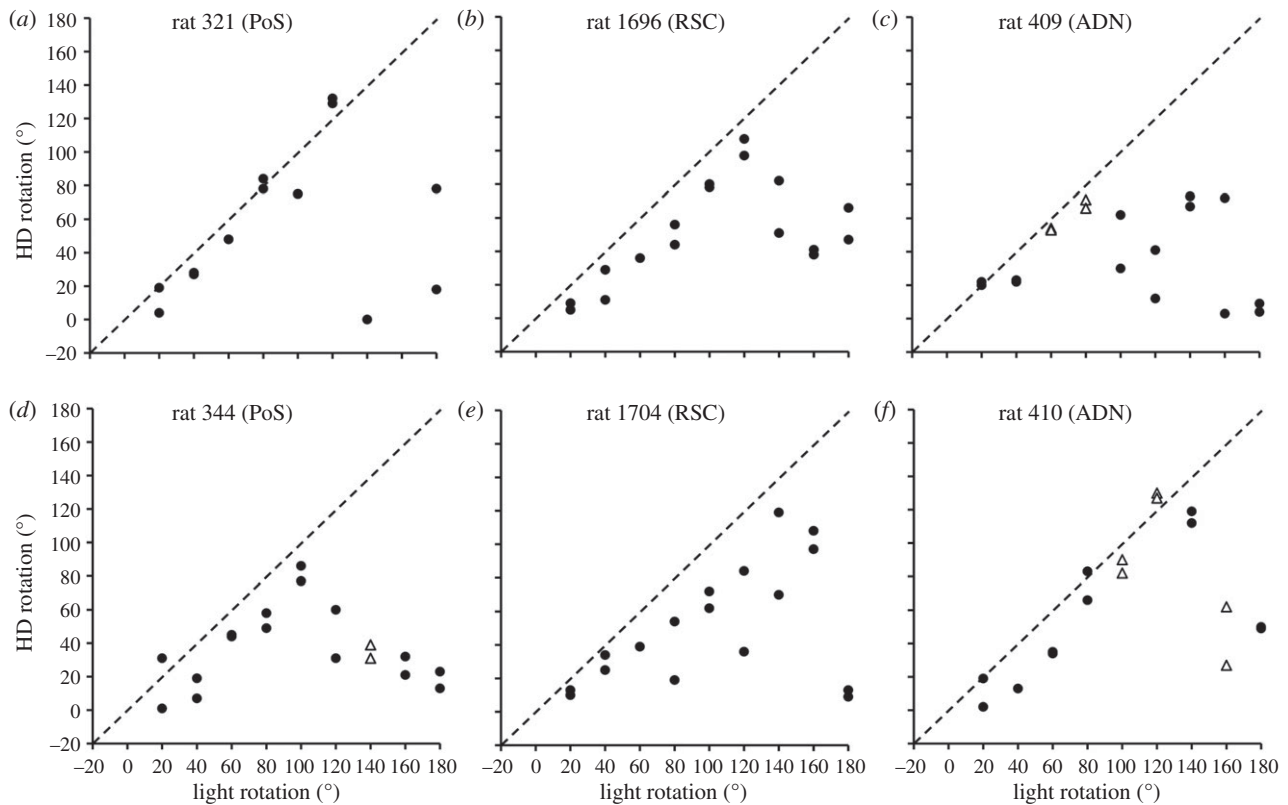


Figure 3. (a–f) Plots showing the breakdown of mean ensemble shifts for each trial within a session in Experiment 1. Separate plots indicate each of the six rats. Each data point represents the mean ensemble shift from one trial to the next. Thus, there are two points for each light rotation (two light shifts per session). The diagonal $y = x$ line indicates the amount the light shifted for each session. The filled circles show rotations in the standard (clockwise) direction, while open triangles indicate the mean ensemble firing shift during the probe trials, when the landmark was rotated in the anticlockwise direction.

Table 1. The table shows the mean shift for all cells per session, expressed both in degrees and as a percentage of the actual light shift. Remaining columns show the absolute mean deviations (mean shift–light rotation), standard error as a % of the light shift, vector length, and results from the Rayleigh test to determine whether they significantly cluster ($*p < 0.05$, $***p < 0.001$).

light shift	ensemble shift (mean)	mean shift (% light shift)	abs. deviation (mean \pm s.e.m. as % of light shift)	vector length 'R'	Rayleigh test (Z)
20°	12.84°	64	7.16° (\pm 9.2)	0.99	5.96***
40°	19.76°	49	20.24° (\pm 8.3)	0.98	5.88***
60°	42.58°	71	17.42° (\pm 4.6)	0.99	5.92***
80°	60.38°	75	19.62° (\pm 7.59)	0.97	5.58***
100°	73.06°	73	26.94° (\pm 5.41)	0.97	5.68***
120°	91.34°	76	28.66° (\pm 14.49)	0.70	2.98*
140°	70.34°	50	69.66° (\pm 10.88)	0.79	3.82*
160°	48.68°	30	111.32° (\pm 6.64)	0.90	4.02**
180°	30.87°	17	149.13° (\pm 4.76)	0.93	5.22**

Taken together, these results suggest that the HD cells used a combination of both the light landmark and the background cues at all conflict sizes. The weighting of this information was, however, dependent on the session. For the first part of the session, the mean firing rotation was approximately the same as the light shift minus a constant offset of around 20°. This pattern showed some variation between animals, with cells in rat 1704 showing more of a tendency to steadily pull away from the light as conflict increased (figure 3). For conflicts past 120°, from the sixth session onwards, the tuning curves suddenly started to drop away substantially in all cases, with

most cells adopting (to varying degrees) intermediate states that showed a steady progression from being closer to the light to closer to the background cues.

Examination of the pattern of responding in individual rats revealed that this compromise between cues occurred within single cells and was not just a population average. The majority of cells adopted intermediate mean firing directions (with the exception of those in rat 321, which showed a more abrupt switch). Thus, for the majority of cells, the intermediate rotation values for the light rotations of 140° and 160° (figure 4) are due to intermediate values expressed

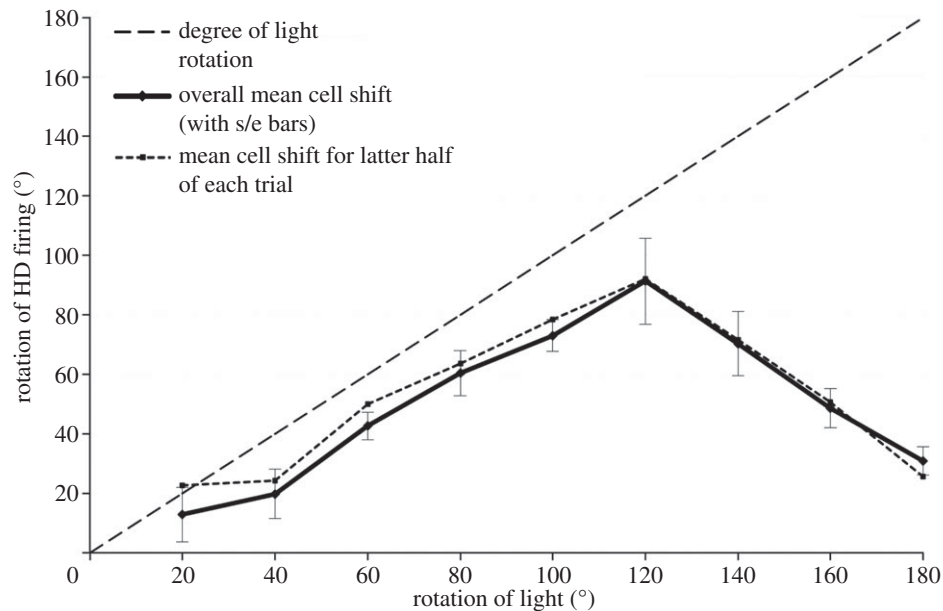


Figure 4. Plot showing the relationship between the expected shifts in degrees of the HD cells based on the light shift (dashed line) and the actual mean ensemble firing shift (solid line; error bars show s.e.m as a % of light shift) across each session. The dotted line represents the actual mean ensemble firing shift using data from only the last 2 min of each trial.

Table 2. Calculations for each light rotation (i.e. each session), comparing the undershoot (absolute deviation) to 0° and the mean ensemble shift to 0°.

light shift	undershoot (mean \pm s.e.m as a % of light)	undershoot different from 0? (upper CI/lower CI) in degrees	mean ensemble shift	mean shift different from 0? (upper CI/lower CI) in degrees
20°	7.16° (\pm 9.2)	yes (11.46/2.86)	12.84°	yes (17.17/8.59)
40°	20.24° (\pm 8.3)	yes (28.07/12.61)	19.76°	yes (27.5/12.03)
60°	17.42° (\pm 4.6)	yes (24.06/10.89)	42.58°	yes (49.27/36.1)
80°	19.62° (\pm 7.59)	yes (34.38/5.16)	60.38°	yes (80.79/45.26)
100°	26.94° (\pm 5.41)	yes (40.12/13.75)	73.06°	yes (85.94/59.59)
120°	28.66° (\pm 14.49)	no (74.48/− 18.33)	91.34°	yes (134.64/35.52)
140°	69.66° (\pm 10.88)	yes (116.31/22.92)	70.34°	yes (114.02/13.75)
160°	111.32° (\pm 6.64)	yes (147.82/74.48)	48.68°	yes (108.29/17.76)
180°	149.13° (\pm 4.76)	yes (170.74/127.77)	30.87°	yes (46.41/9.74)

across all trials and not to a combination of trials where cells rotated fully with the light and trials where they completely failed to rotate.

(ii) Probe trials

The progressively increasing under-rotation of the firing directions may be due to one or both of two factors. The first is that perhaps the system learned about a steadily increasing uncertainty concerning the location of the light, based on the repeated conflicts with the background cues: in other words, it learned that the light could not be trusted as a reliable indicator of direction, so that the light failed to capture the cells. The other is that perhaps the system always trusted the light, but gradually learned a new association between the light and the directional system. That is, perhaps the light always captured the cells but the relationship between the light and the cells changed across time. We tested this possibility by introducing probe trials in three animals in which the light was unexpectedly moved in the opposite direction, anticlockwise instead of the usual

clockwise. If the cells had simply learned that the light was uncertain (had a broad variance), they should under-rotate in these probes just as they under-rotated following rotations in the usual direction. If they had learned a new mapping, then on these reverse trials they should over-rotate, to maintain the same position with respect to the light. The results of these probes are shown by the open triangles in figure 3. It is evident that in these counter-rotation probes, the cells show the amount of under-rotation that would be predicted on the basis of the data points on either side. Thus, it seems unlikely that the cells learned a new mapping—rather, they seem to have simply learned a weaker influence. This is discussed further in the next section.

(b) Experiment 2

In this experiment, rats were exposed to the same conflict protocol, but only a single conflict size—140°—was used. Using the same inclusion criteria as for Experiment 1, we selected for analysis a total of five individual HD cells, in four ensembles of one and two cells in each. These five

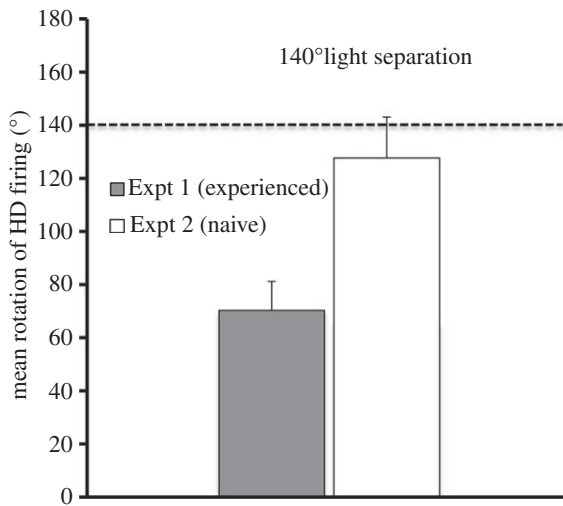


Figure 5. Plot comparing the mean (\pm s.e.m.) ensemble firing shift of HD cells from Experiment 1 and Experiment 2 during a 140° light shift. The dashed line indicates the degree of light rotation (140°).

cells were recorded from three rats during seven sessions of 35 trials. Across all five cells, the average peak firing rate was 22.98 Hz (± 8.96), the average firing range was 164.18° (± 103.25) and the average 'R' value was 0.4.

(i) Cue conflict trials

By contrast with Experiment 1, the switching on of the light at 140° in these initially naive rats produced strong cue-following—cells rotated their mean firing direction close to 140° on all trials (figure 5). The deviation in mean firing rotation from the actual light rotation (140°) was not significantly greater than zero (upper CI = 53.86, lower CI = -26.36). Statistical analysis of the ensemble activity showed that all data points are significantly clustered (Rayleigh test, $z = 3.92$, $p < 0.05$), suggesting that all the recorded HD cells, across all trials, rotated their firing by similar amounts when exposed to the 140° light conflict. A Watson–Williams test [23] showed that there was a significant difference in the mean firing shift during Experiment 1 and those trials in Experiment 2 when the light shifted by 140° , $F_{1,11} = 6.52$, $p < 0.05$. We can therefore conclude that in Experiment 1 at a 140° light conflict, HD cells (that had previously been exposed to smaller light conflicts) significantly under-rotated. However in Experiment 2, where HD cells had not previously been exposed to smaller light conflicts, the tuning curve rotation did not deviate significantly from the light cue rotation at 140° .

4. Discussion

The present experiment examined how HD cells responded to a conflict between two cue sets: background cues (including self-motion cues and uncontrolled environmental cues) versus a highly salient landmark cue. We found that the cells responded not by 'cue capture', a winner-take-all process in which they followed the strongest cue set, but rather in an integrative fashion in which the cells adopted a firing direction intermediate between the directions signalled by the two cue sets. Furthermore, the position of the compromise firing direction shifted with amount of conflict and/or experience, being close to the visual cue initially, and close to the background cues towards the end of the conflict series. The weighting of

the background cues was much less in naive animals, suggesting a contribution of experience to the decision process.

'Under-rotation' of HD cells in response to cue rotation has been reported in a number of previous studies, and indeed seems to be a highly reliable finding in cue conflict experiments. In the original study of cue control of HD cells by Taube *et al.* [3], two cells tested with cue card rotation done while the animals were present in the environment showed under-rotation. A number of more recent studies have found similar results [3,4,7,11–18]. For example, Taube & Burton [7] explicitly introduced a conflict between a cue card and the rat's current sense of direction, and found that although the HD signal was somewhat corrected by the cue, there was an under-rotation of around 20° , suggesting a contribution from both the previous HD orientation and the (now-rotated) landmark. A summary of the studies in which responding to a rotated cue has been examined is presented in table 3. Although the amount of under-rotation varies, presumably as a function of other factors like whether and how much the rats were disoriented, or how salient the other cues were, it is nevertheless a highly consistent finding that rotation of a cue rarely results in complete cue-following.

The additional contribution made by our study is that under-rotation is not constant but varies as a function of the experience of the animal; in animals exposed to repeated and gradually increasing cue conflicts the cells suddenly began to increase their under-rotation, while a similar degree of conflict in naive animals yielded much less undershoot (figure 5), indicating plasticity in the system.

It is not fully straightforward to explain these findings. On the one hand, it seems natural that when there are conflicting cues, a sensory system should respond in a compromise manner, expressing contributions from both sets of cues. On the other hand, how could such integrative dynamics arise from an attractor network? Why does the signal rotate partly towards the cue but then stop? Why does not the cue, which is constantly present, 'drag' activity in the network all the way around until the conflict is eliminated? (Or conversely, if the competing cues are very strong, fail to drag it at all?). The settling of the HD system to a position short of complete reorientation suggests that some kind of plasticity must have occurred, reweighting the visual cue dynamically during the trial, so that by the end it has a slightly different relationship with the HD signal. In the electronic supplementary material, and also in the companion paper to this one [10], we explore this issue in detail, outlining how plasticity in an attractor network can lead to integrative behaviour and presenting some simulations of this process. According to our hypothesis, rapid intratrial reweighting of the inputs from the landmark onto the (putative) ring attractor would result in the activity of the HD network stabilizing at a point intermediate between the two excitatory drives onto the ring (the one from the landmark via the visual system and the other from the background cues; electronic supplementary material, figure S2). The amount of integration would depend on the speed of reorientation, which in turn would depend on the strength of the sensory drive. For a very strong drive from, say, the visual landmark, reorientation would be rapid and reweighting would have little time to occur, leading to activity progressing almost all the way around the ring to be captured by the visual cue. Indeed, Redish [27] has discussed how a very strong cue could cause activity to disappear from the original location on the ring and reappear at the location of the cue, without moving

Table 3. Summary of the literature on cue conflict experiments with HD cells.

study	relevant manipulation	HD response
Taube <i>et al.</i> [1,3]	cue card rotated stepwise with animal <i>in situ</i>	two cells tested in four trials—under-rotation of approximately 30°–60°
Taube & Burton [7]	rat walked between familiar cylindrical compartment containing cue card, through novel passageway to novel rectangular compartment, and then returned. Sometimes, before return, the cue card in the cylinder was rotated 90°	when cue card rotated by 90°, cells ($n = 24$) under-rotated by around 20°
Taube [25]	rat removed from chamber while cue card rotated $\pm 90^\circ$, or 180°, rat mildly disoriented before being replaced	HD cells in the ADN showed a deviation from expected shift of around 13°, with a tendency to under-rotate (10 under-rotations and three over-rotations)
Goodridge & Taube [4]	rat removed from cylinder and mildly disoriented, replaced in cylinder, then cue card re-introduced at a position conflicting with current HD orientation, which was either (i) the original location or (ii) 90° rotated	(i) when cue card returned to original position, cells returned to within 7° of original heading direction. (ii) When card returned to rotated position, cells rotated towards card but under-rotated by around 40°
Knierim <i>et al.</i> [12]	place and HD cells recorded in a cylinder with a cue card that was rotated from trial to trial; rats were (i) disoriented or (ii) not disoriented before being placed in the apparatus on each trial	for both groups, rotation of the cells occurred to within 15° of card rotation, but the probability of complete disconnection from the card was increased in the disorientation-trained rats
Dudchenko <i>et al.</i> [15]	rat removed from recording cylinder and mildly disoriented, meanwhile floor paper changed and cue card rotated 90°. (clockwise in first session, anticlockwise in second session)	15 rotations tested in each direction; cells showed under-rotation, but only of around 10°
Goodridge <i>et al.</i> [18]	rats exposed to a novel cue card for (i) a short time (1 min), or (ii) a longer time (8 min), the rat then removed and disoriented, floor paper changed, etc., while the card was rotated 90°, rat was reintroduced	(i) (Their fig. 7B.) Eight HD cells showed mixed reaction (some cells rotating more than others) with a mean under-rotation of around 45°. (ii) (Their fig. 7A.) Five cells tested and found to under-rotate by around 20°, similar to rotation of a familiar cue card in Taube <i>et al.</i> [1,3] and Taube [25]
Zugaro <i>et al.</i> [16]	with rat present, wall and cue card rotated 45°, 90° or 180°	a small but significant under-rotation of PoS and ADN HD cells of around 10%
Zugaro <i>et al.</i> [17]	three evenly spaced objects at the periphery of a walled-off circular arena were rotated 120° in the absence of the rat; rat mildly disoriented before replacement	mild tendency to under-rotation; in 21 sessions the cells rotated less than the objects, in nine sessions they over-rotated; mean shift of around 5° less than the cues
Yoganarasimha <i>et al.</i> [13]	in a curtained-off arena with a central circular track, distal cues were rotated (while rat in a covered box) twice; (i) 45° clockwise and (ii) in a second session, an additional 45° clockwise. Rat mildly disoriented before being replaced on the track	(i) place and HD cells under-rotated by around 10°–15°. (ii) The cells rotated close to 45°
Clark <i>et al.</i> [26]	cue card rotated 90° clockwise or anticlockwise with rat not present; rat mildly dosoriented before being replaced	19 HD cells under-rotated by around 15°

through intermediate locations on the ring at all, a proposition for which there is some experimental support [28]. Such behaviour would look like complete cue capture, with no integrative behaviour resulting. For a weaker landmark (one that had, for example, been experienced as unstable) then reorientation would be slower, reweighting would have more time to occur and activity would be integrative, assuming a final state that was further from that weaker cue.

An interesting property emerges from this hypothetical intratrial reweighting process, which is that it provides a method for weighted cue integration, in which the contribution of a sensory cue to a decision about the real world is weighted by the information, or reliability, possessed by the cue. Weighted cue combination has been a topic of considerable interest in the sensory integration community for many years but a biologically plausible neural mechanism has not been

forthcoming. In the electronic supplementary material, we explore the possibility that short-term plasticity in an attractor network may provide such a mechanism, and thus a method for making optimal decisions about imperfect or conflicted sensory information. We present a simulation of this proposal in a separate paper [10] and find not only weighted cue combination, but also the discontinuity seen in the HD cell responding when the conflict exceeds a certain level.

Our proposed network also possesses another property, which is that longer-term plasticity in the inputs from the landmark provides a mechanism for *new* learning about reliability. Several previous studies have found that HD and place cells' responsiveness to a cue card is altered when the relationship between the cue and the internal sense of direction changes—for example, Knierim *et al.* [12] found that in rats that had been repeatedly disoriented prior to recording, HD cells and place cells were less likely to follow a cue card. The interpretation placed on this observation was that in disoriented rats, the variable relationship of the cue card to the HD signal caused the card to be treated as an unreliable landmark. Goodridge *et al.* [18] found that a cue card controlled HD reorientation if the rats had had 8 min of experience that the cue was stable, but much less so if they had only seen the cue for a minute [18], again suggesting that experience of stability/reliability is an important determinant of cue control.

How might 'reliability' be encoded in a neural network? One possibility is in the form of the strength and distribution of weights from the visual neurons to the HD cells. When reliability is high, then as suggested above, projections would be strong and only distributed over a narrow band of HD cells. When reliability is lower, e.g. because the rat has experienced instability of the visual cue, then the weights would be weaker and distributed over a larger range of HD cells. As a result, the pull from the visual drive would shift activity around the ring less quickly, allowing more time for reweighting and resulting in a greater final level of undershoot. Thus, between-trial

reweighting provides a mechanism for cue *learning* (as distinct from within-trial plasticity for cue integration).

What could be the adaptive advantage of learned reliability-weighted averaging in the HD system? Under what circumstances could a landmark vary in reliability? Surely, an object in the world is either mobile, in which case it is useless as a landmark, or immobile, in which case it is fully reliable? One possibility has to do with the bootstrapping process by which we envisage that the HD system learns about cue configurations. Although stable landmarks do not vary in their allocentric direction, they may vary in how their direction is represented in the HD network, which has to learn the direction of a landmark based on its own current still-being-established HD signal. Before the signal itself is highly reliable, the system has to independently adjust the weightings of the landmarks and/or its own relationship to the cue constellation, until stability is achieved. It may be that the cue integration that we observed is a reflection of this bootstrapping process.

To conclude, then, our experiments show that HD cells resolve cue conflicts in a weighted manner, finding a stable endpoint that is located between the two component cue sets. The variable location of the endpoint suggests a weighted decision process, which could arise from plasticity in an attractor network. Our conclusion is that the ingredients for reliability-weighted cue integration are, in principle, present in the HD attractor network and perhaps in other sensory systems also.

Acknowledgements. The authors are grateful for technical help from Jim Donnett (Axona Ltd), analysis help from Robin Hayman and useful discussion and comments from Maarten Speekenbrink.

Funding statement. K.J.J. was supported by grants from the European Commission Framework 7 ('Spacebrain') and the Medical Research Council (G1100669). R.K. and E.M. were supported by studentships from the Biotechnology and Biological Sciences Research Council (BBSRC).

References

1. Taube JS, Muller RU, Ranck Jr JB. 1990 Head-direction cells recorded from the postsubiculum in freely moving rats. I. Description and quantitative analysis. *J. Neurosci.* **10**, 420–435.
2. Taube JS. 2007 The head direction signal: origins and sensory-motor integration. *Annu. Rev. Neurosci.* **30**, 181–207. (doi:10.1146/annurev.neuro.29.051605.112854)
3. Taube JS, Muller RU, Ranck Jr JB. 1990 Head-direction cells recorded from the postsubiculum in freely moving rats. II. Effects of environmental manipulations. *J. Neurosci.* **10**, 436–447.
4. Goodridge JP, Taube JS. 1995 Preferential use of the landmark navigational system by head direction cells in rats. *Behav. Neurosci.* **109**, 49–61. (doi:10.1037/0735-7044.109.1.49)
5. Zugaro MB, Arleo A, Dejean C, Burguiere E, Khamassi M, Wiener SI. 2004 Rat anterodorsal thalamic head direction neurons depend upon dynamic visual signals to select anchoring landmark cues. *Eur. J. Neurosci.* **20**, 530–536. (doi:10.1111/j.1460-9568.2004.03512.x)
6. Stackman RW, Golob EJ, Bassett JP, Taube JS. 2003 Passive transport disrupts directional path integration by rat head direction cells. *J. Neurophysiol.* **90**, 2862–2874. (doi:10.1152/jn.00346.2003)
7. Taube JS, Burton HL. 1995 Head direction cell activity monitored in a novel environment and during a cue conflict situation. *J. Neurophysiol.* **74**, 1953–1971.
8. Skaggs WE, Knierim JJ, Kudrimoti HS, McNaughton BL. 1995 A model of the neural basis of the rat's sense of direction. *Adv. Neural Inf. Process Syst.* **7**, 173–180.
9. Boucheny C, Brunel N, Arleo A. 2005 A continuous attractor network model without recurrent excitation: maintenance and integration in the head direction cell system. *J. Comput. Neurosci.* **18**, 205–227. (doi:10.1007/s10827-005-6559-y)
10. Page HJ, Walters DM, Knight R, Piette CE, Jeffery KJ, Stringer SM. 2014 A theoretical account of cue averaging in the rodent head direction system. *Phil. Trans. R. Soc. B* **369**, 20130283. (doi:10.1098/rsta.2013.0283)
11. Taube JS. 1995 Place cells recorded in the parasubiculum of freely moving rats. *Hippocampus*. **5**, 569–583. (doi:10.1002/hipo.450050608)
12. Knierim JJ, Kudrimoti HS, McNaughton BL. 1995 Place cells, head direction cells, and the learning of landmark stability. *J. Neurosci.* **15**, 1648–1659.
13. Yoganarasimha D, Yu X, Knierim JJ. 2006 Head direction cell representations maintain internal coherence during conflicting proximal and distal cue rotations: comparison with hippocampal place cells. *J. Neurosci.* **26**, 622–631. (doi:10.1523/JNEUROSCI.3885-05.2006)
14. Clark BJ, Taube JS. 2011 Intact landmark control and angular path integration by head direction cells in the anterodorsal thalamus after lesions of the medial entorhinal cortex. *Hippocampus* **21**, 767–782. (doi:10.1002/hipo.20874)
15. Dudchenko PA, Goodridge JP, Taube JS. 1997 The effects of disorientation on visual landmark control of head direction cell orientation. *Exp. Brain Res.* **115**, 375–380. (doi:10.1007/PL00005707)

16. Zugaro MB, Tabuchi E, Wiener SI. 2000 Influence of conflicting visual, inertial and substratal cues on head direction cell activity. *Exp. Brain Res.* **133**, 198–208. (doi:10.1007/s002210000365)
17. Zugaro MB, Berthoz A, Wiener SI. 2001 Background, but not foreground, spatial cues are taken as references for head direction responses by rat anterodorsal thalamus neurons. *J. Neurosci.* **21**, RC154.
18. Goodridge JP, Dudchenko PA, Worboys KA, Golob EJ, Taube JS. 1998 Cue control and head direction cells. *Behav. Neurosci.* **112**, 749–761. (doi:10.1037/0735-7044.112.4.749)
19. Knierim JJ, Kudrimoti HS, McNaughton BL. 1998 Interactions between idiothetic cues and external landmarks in the control of place cells and head direction cells. *J. Neurophysiol.* **80**, 425–446.
20. Rotenberg A, Muller RU. 1997 Variable place-cell coupling to a continuously viewed stimulus: evidence that the hippocampus acts as a perceptual system. *Phil. Trans. R. Soc. Lond. B* **352**, 1505–1513. (doi:10.1098/rstb.1997.0137)
21. Knight R, Hayman R, Jeffery K. 2011 Geometric cues influence head direction cells only weakly in nondisoriented rats. *J. Neurosci.* **31**, 15 681–15 692. (doi:10.1523/JNEUROSCI.2257-11.2011)
22. Van der Meer MA, Richmond Z, Braga RM, Wood ER, Dudchenko PA. 2010 Evidence for the use of an internal sense of direction in homing. *Behav. Neurosci.* **124**, 164–169. (doi:10.1037/a0018446)
23. Berens P. 2009 CircStat: a MATLAB toolbox for circular statistics. *J. Stat. Softw.* **31**, 1–21.
24. Paxinos G, Watson C. 2004 *The rat brain in stereotaxic coordinates*. New York, NY: Academic Press.
25. Taube JS. 1995 Head direction cells recorded in the anterior thalamic nuclei of freely moving rats. *J. Neurosci.* **15**, 70–86.
26. Clark BJ, Harris MJ, Taube JS. 2010 Control of anterodorsal thalamic head direction cells by environmental boundaries: comparison with conflicting distal landmarks. *Hippocampus* **22**, 172–187. (doi:10.1002/hipo.20880)
27. Redish AD. 1999 *Beyond the cognitive map: from place cells to episodic memory*. Cambridge, MA: MIT Press.
28. Zugaro MB, Arleo A, Berthoz A, Wiener SI. 2003 Rapid spatial reorientation and head direction cells. *J. Neurosci.* **23**, 3478–3482.